Miniaturized PMUT-Based Receiver for Underwater Acoustic Networking

Bernard Herrera[©], Graduate Student Member, IEEE, Flavius Pop[©], Graduate Student Member, IEEE, Cristian Cassella[©], Member, IEEE, and Matteo Rinaldi[©], Senior Member, IEEE

Abstract—The present work reports on the novel implementation of a miniaturized receiver for underwater networking merging a Piezoelectric Micromachined Ultrasonic Transducer (PMUT) array and signal conditioning circuitry in a single, packaged device. Tests in both a large water tank and a pool demonstrated that the system can attain large enough Signalto-Noise Ratio (SNR) for communication at distances beyond two meters. An actual communication test, implementing an Orthogonal Frequency Division Multiplexing (OFDM) scheme, was used to characterize the performance of the link in terms of Bit Error Rate (BER) vs SNR. In comparison to previous work demonstrating high-data rate communication for intra-body links and acoustic duplexing, this implementation allows for significantly larger distances of transmission, while addressing the signal conditioning and submersible packaging needs for underwater conditions, thus enabling PMUT arrays for operating as complete underwater communication receivers. [2020-0185]

Index Terms—PMUT, ultrasonic, underwater, direction of Arrival, AVS.

I. INTRODUCTION

THE "Internet of Underwater Things" (IoUT), the system technology focus of this work (Fig 1), is an active research field with promising applications in environmental monitoring, exploration and disaster prevention, given its ability to collect underwater network data and re-transmit it to shore or satellites via Radio Frequency [3]. The transducers that provide the physical layer of the acoustic link in this communication network are generally bulk transducers based on Lead Zirconium Titanate (PZT). Well established and commercially available devices exist implementing transceiver functionalities such as acoustic modems [4]–[6]. These devices integrate a piezoelectric transducer used as a transceiver and modulation circuitry and are able to implement communication links with distances in a range between hundreds of meters to kilometers with relatively low data rates (Table III).

Other type of devices of interest within the frame of the IoUT are Acoustic Vector Sensors (AVSs), given their

Manuscript received May 15, 2020; revised July 27, 2020; accepted July 28, 2020. Date of publication September 1, 2020; date of current version October 7, 2020. This work was supported in part by the NSF Programs MRI-SEANet under Grant NSF 1726512 and in part by the NeTS-Medium under Grant NSF 1764055. Subject Editor M. Rais-Zadeh. (Corresponding author: Bernard Herrera.)

The authors are with the Department of Electrical and Computer Engineering, Northeastern University, Boston, MA 02118 USA, and also with the Northeastern SMART Center, Northeastern University, Boston, MA 02118 USA (e-mail: herrerasoukup.b@northeastern.edu).

Color versions of one or more of the figures in this article are available online at http://ieeexplore.ieee.org.

Digital Object Identifier 10.1109/JMEMS.2020.3018070

capabilities for acoustic signal enhancement and Direction of Arrival (DOA) estimation [7]. Large form factor Commercial Off-The-Shelf (COTS) devices implementing these functionalities exist such as acoustic ranger-locator combinations ("Underwater GPS" [8]) or Directional Acoustic Transducers [9]. Similarly to acoustic modems, these devices can operate at ranges of several kilometers. Miniaturized AVS implementations have also been explored but are reserved to measurements in air such as a thermal difference-based sensor [10], an acoustic camera [11] or a DOA estimation system based on orthogonal microphones [12]. An exception suitable for underwater DOA estimation, also being the only Micro Electro Mechanical System (MEMS) implementation, is a sensor bio-inspired on fish organs [13]. However, these miniaturized examples serve as a proof of concept and have not been demonstrated beyond short range laboratory conditions.

On the other hand, recent research has showcased Piezoelectric Micromachined Ultrasonic Transducers (PMUTs) as transducers with a better acoustic matching to the liquid medium, with a consequent larger bandwidth [14], in comparison with bulk transducers. This feature has proven to be able to significantly improve the performance of ultrasonic underwater networking schemes [15]. This is why, even though PMUTs have been typically investigated in in-air range-finding [16], fingerprint scanning [17], imaging [18] and gesture recognition [19], their exploration as underwater transceivers is of interest. Previous work from the authors has implemented related functionalities such as high-data rate communication for intrabody links [1] and acoustic duplexing [2].

Additionally, in comparison to single, bulk transducers, PMUTs can be fabricated into large arrays due to their small size and fabrication versatility. Thus, they can offer capabilities similar to AVSss as beamforming and source localization [20] in a comparable or smaller footprint.

However, the tradeoff to the advantages offered by PMUTs is their generally small signal output at considerable distances as compared to bulk transducers. Published research addressing this challenge has been limited to device optimization for underwater operation [21]. The present work aims to take one step further by tackling the signal conditioning and packaging of the devices into a full acoustic networking receiver. Thus, the actual communication capabilities and range of PMUT-based transceivers can be enabled.

II. METHODOLOGY

A representative fabricated PMUT array was used to show-case the approach of the current work for custom signal

1057-7157 © 2020 IEEE. Personal use is permitted, but republication/redistribution requires IEEE permission. See https://www.ieee.org/publications/rights/index.html for more information.

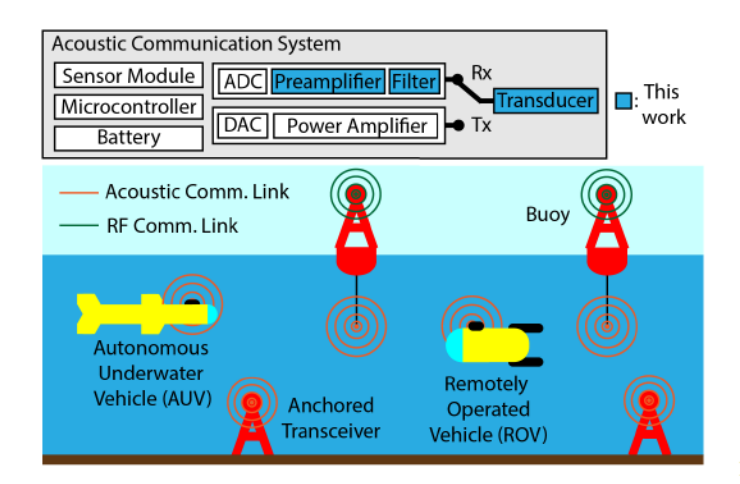


Fig. 1. Envisioned application: Ultrasonic transceivers enable the creation of acoustic underwater networks. Within the different components of the transceiver system, the present work delivers an encapsulated receiver including a PMUT array transducer and signal conditioning circuits.

conditioning, packaging and test results. However, PMUT arrays with varying number of elements, cavity dimensions and pitch between elements are subject to the method. This allows flexibility for engineering parameters such as operating frequency, which has a direct effect on acoustic loss, range and bandwidth, or array characteristics, that affect acoustic directivity.

A. PMUT Array

The fabrication included a rectangular array of Aluminum Nitride (AIN) PMUTs arranged in a channel configuration (Fig. 2). This configuration allows for flexibility in the operation of the device. If all the channels are electrically connected in parallel, the output of all the individual elements are joined and thus, the working range of the device is maximized. If, instead, the signals are treated separately as they arrive to the separated channels, beamforming and source localization capabilities are enabled [20].

The transducer stack consists of an AlN layer located between gold and platinum top and bottom electrodes, respectively. Deep Reactive Ion Etching (DRIE) is used to etch cavities through the wafer and release the circular membranes. The fabrication process is the same as described in [20]. Once the wafer is fabricated and diced into individual chips, a chip is wire-bonded to a custom PCB with the signal conditioning circuitry on its backsede. Finally, the assembly is coated in a flexible layer of Polydimethylsiloxane (PDMS) by dipping and curing (Fig. 2).

B. Signal Conditioning

Charge amplifier circuits were specifically designed to properly interface with the impedance of the PMUT array while taking full advantage of the large bandwidth the transducers provide (Fig 5). The charge amplifier topology is optimal for interfacing with the PMUT array as it is particularly designed to amplify charge rather than voltage. In this manner, the small charges produced by the piezoelectric effect for

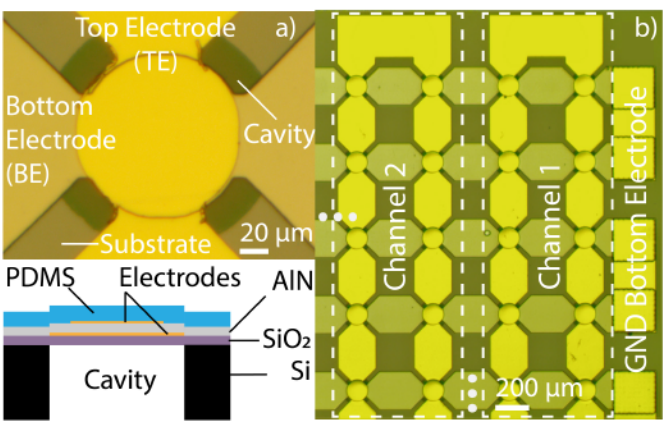


Fig. 2. a) Schematic of the layer stack and optical micrograph of a PMUT element. b) Schematic and optical micrograph of a portion of the fabricated array. Blocks of 20 PMUTs are connected in parallel forming individual channels and these channels can be further joined together to maximize the output of the full array.

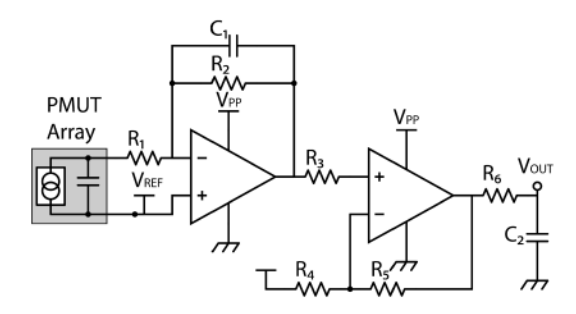


Fig. 3. Schematic of the signal conditioning circuitry. The circuit consists of a first OpAmp stage providing charge to voltage conversion (integrator). A second stage, with an OpAmp in a non-inerting amplifier configuration, provides additional gain. An RC filter is placed before the output to provide further noise filtering.

the expected faint acoustic signals at considerable distances, can be converted into levels readable by standard electronic circuits. The circuits consist of an OpAmp stage working as a capacitive integrator (providing the charge to voltage conversion) and a second stage purely providing voltage gain (Fig. 3).

The frequency response of the circuit also provides noise filtering advantages. The combination of the PMUT array's static capacitance C_0 and R_1 produces a low-pass pole that mitigates high-frequency noise. C_1 and R_2 form a high-pass zero that reduces the low-frequency noise. An additional low pass filter, formed by R_6 and C_2 adds to the high frequency noise filtering and increases the slope of the high frequency roll-off (Fig. 5). Depending on the desired center frequency and bandwidth of operation, the circuit components can be modified to achieve a desired gain and pass-band frequencies.

It is important to note that OpAmps with a high gain-bandwidth product must be selected, as small charges are to be amplified within a considerable bandwidth. Low spectral noise power is another important specification required for the OpAmps to maintain the SNR levels. Low bias currents and high input impedance are also desirable characteristics in order to match the corresponding high output impedance from the transducer [22].

C. Device Packaging

A custom-designed Printed Circuit Board (PCB) combined the PMUT array chip on one side with the signal conditioning circuitry on the other. On the PMUT array side, the chip was adhered to the PCB and electrical connections were established through wire-bonds. Surface-Mount Device (SMD) components were soldered on the reverse and connected to the array output through vias.

The flexible polymer Polydimethylsiloxane (PDMS) then encapsulated the assembly (Fig 2), providing both water-proofing and mechanical protection for the delicate wire-bonds and PMUT membranes. The addition of this layer also has the advantage of not significantly impacting the receiving performance as its acoustic impedance is similar to the one of water [23].

D. Test Setup

Before testing the device in long-distance applications, its performance was assessed, while acting as the receiver in an underwater communication link. A reference PZT transducer acted as a transmitter and was placed 40 cm away from the PMUT receiver, both immersed in a water tank. The available bandwidth of the communication channel was characterized by sending an impulse signal to the transmitter and obtaining the Fast Fourier Transform (FFT) of the output signal on the PMUT receiver (Fig. 5).

Once the available bandwidth was determined, a Software Defined Radio (SDR) was used to implement an Orthogonal Frequency Division Multiplexing (OFDM) communication protocol on the transducer. The SDR used in this work is an Ettus Research N210 [24], which is based on an Field-Programmable Gate Array (FPGA) and can be programmed from a personal computer. This protocol takes advantage of the available bandwidth of the physical link by multiplexing data to be transmitted by distributing it in smaller frequency divisions of the band. The SDR provides flexibility in assigning the bandwidth for the transmission as well as the number and width of the sub-carriers within. One SDR implemented the modulation on the transmitter while a second one performed de-modulation on the receiver based on the same protocol and parameters as the transmitter. The modulation scheme used within in each frequency sub-carrier was Binary Phase-Shift Keying (BPSK).

The performance of the link is characterized by the BER obtained by comparing the sent and received bits of a known sequence. However, the BER can be arbitrarily increased by increasing the transmitted power as the signal increases but the noise level remains constant. Thus, the performance was fully characterized by a BER vs SNR curve. Different SNR levels were implemented by changing the transmitting power.

The maximum distance range at which the device can receive a signal level acceptable for implementing successful communication was then tested in two scenarios: a large water tank and a swimming pool (Fig. 4). For these tests, a reference transducer again served as a transmitter and the assembled PMUT device served as a receiver. A 10-cycle burst was sent to the transmitter, the received signal was measured through

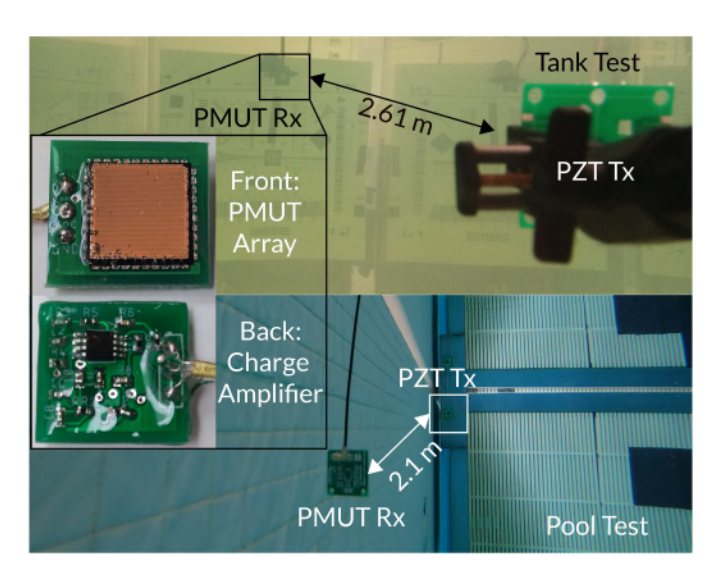


Fig. 4. Tank (top) and pool (bottom) acoustic transmission test setups, a reference transducer was used as a transmitter. Zoom overlay: Front (PMUT array) and bottom (circuitry) faces of the packaged device. Note the PDMS encapsulation. The values of the charge amplifier circuit were designed for the particular transducer to amplify its small output charges and to interface with its capacitance without restricting the bandwidth of operation.

TABLE I SIGNAL CONDITIONING CIRCUIT PARAMETERS

Symbol	Parameter	Value	Units
f_0	Resonant frequency	700	kHz
r	Cavity radius	46	μm
N	Number of elements	50x50	-
C_0	Total static capacitance	1.56	ηF
h,l,t	Chip dimensions	10, 10, 0.3	mm

an oscilloscope and its SNR was estimated by comparison with the noise level. The transmit power on the reference PZT transducer was 36 mW (when driven at 6.55 V_{rms}).

III. RESULTS

For the particular device implemented, the charge amplifiers were designed to provide a large 74 dB gain on a 3dB passband ranging from 70 kHz to 3.17 MHz (Fig. 5). The relevant parameters for the array are summarized in Table I while the circuit values are shown in Table II

Fig. 5 shows the system's frequency response obtained from the FFT of the impulse response. A wide, $200 \ kHz$ $-3 \ dB$ bandwidth was measured around a center frequency of $700 \ kHz$. It is worth noting that the bandwidth is limited by the transmitting reference transducer's frequency response. The PMUT receiver actually has a wider pass-band.

The results of the long distance burst tests are shown in Fig. 6. As the speed of sound in the water is known, and the time delay from the Tx burst to the received signal can be measured through the oscilloscope, the distance can be precisely calculated from these two values. The test across the length of the large water tank showed a received signal SNR of 21 dB at a distance of 2.71 m, while the swimming pool test resulted in a smaller SNR of 11 dB due to added noise and motion artifacts (Fig. 4, Fig. 6).

TABLE II
SIGNAL CONDITIONING CIRCUIT PARAMETERS

Symbol	Value	Units
R_1	1	$k\Omega$
R_2	100	$k\Omega$
C_1	0.1	pF
R_3	270	Ω
R_4	1	$k\Omega$
R_5	50	$k\Omega$
R_6	50	Ω
C_2	680	pF
OpAmp	LT1886	_
\widehat{GBW}^{1}	720	MHz
e_n^{-2}	2.75	$\eta V/\sqrt{Hz}$
P^{3}	70	mW

- OpAmp Gain-Bandwidth Product
- ² OpAmp Spectral Noise Density
- ³ Circuit Power Consumption

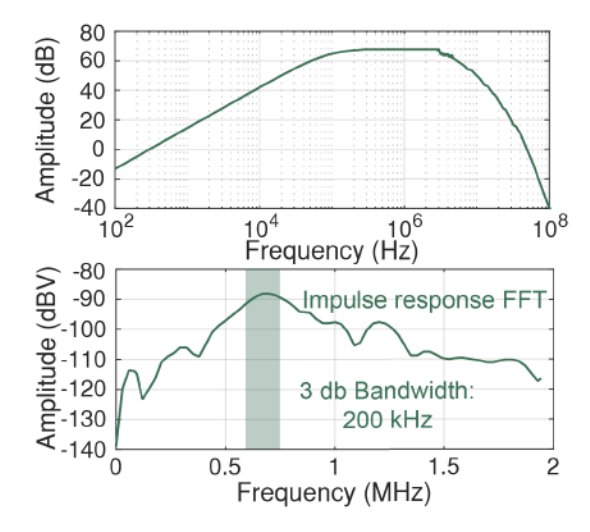


Fig. 5. Top: Simulated gain of the charge amplifier taking into account the PMUT array capacitance. While offering a high gain and impedance matching for the array, the circuit is designed to filter off-band noise. Bottom: System frequency response. Fast Fourier Transform (FFT) of the time-domain impulse response from a reference transducer, through a water medium to the PMUT array. A wide 200 kHz 3 dB bandwidth is a result of the good matching of PMUTs to the medium.

The reason for the chosen frequency of operation (700 kHz) is related to a trade-off between smaller acoustic attenuation at lower frequencies and wider bandwidth at higher ones. Fabrication difficulties prevent achieving resonant frequencies below approximately 300 kHz. For very large transmitting distances, reducing the operating frequency to this limit value would have a significant impact in terms of reduced acoustic attenuation. However, based on the attenuation formula for water [25] at the distance implemented in this work, shifting from 700 to 300 kHz would only signify an increase of SNR of around 0.2 dB. The advantage gained from the lower attenuation would also come at the cost of a reduced bandwidth.

Fig. 7 details the data obtained for the BER vs SNR characterization for the implemented OFDM protocol. The BER decreases linearly, on a logarithmic plot, as SNR increases as expected. The SNR levels obtained in the tank and pool tests,

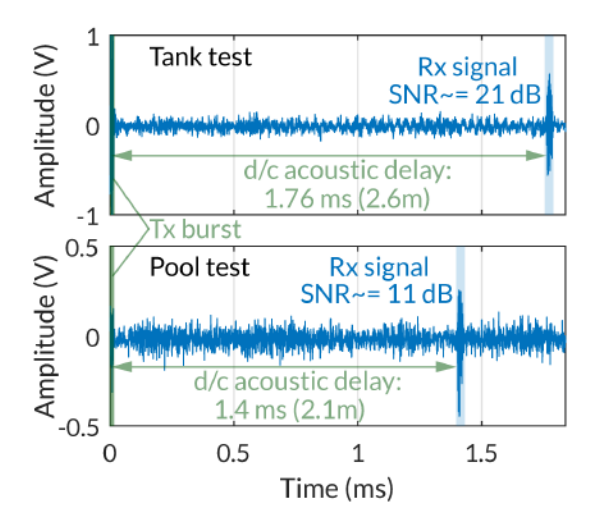


Fig. 6. Time domain burst transmission tests. Top: tank test. Bottom: Pool test. The measurements correspond to the output of the whole array connected in parallel.

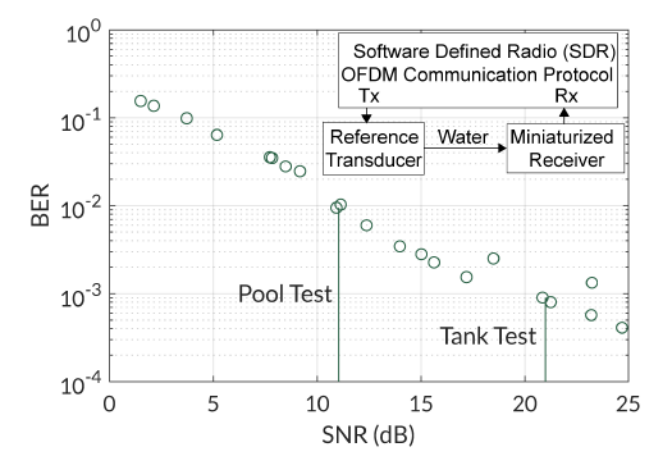


Fig. 7. Communication test. A Software Defined Radio (SDR) implemented an OFDM communication protocol which spreads data subcarriers across the available spectrum, thus benefitting from the large bandwidth provided by the PMUT receiver. Transmitted power was swept at a fixed distance, changing the SNR at the receiver. BER was measured for every sweep point by checking for errors on a preset sequence. The SNR levels, and the BERs they would correspond to for the pool and tank test are marked. The BERs obtained prove the system suitable for underwater communication.

from the burst tests, are marked on the graph to determine the BER levels that can be achieved for each. Such results proved the applicability of the receiver in an underwater link by achieving a Bit Error Rate (BER) of less than 9×10 -4 for the SNR obtained in the tank test (Fig 7).

The reason for the low BERs obtained is indicative of the wide bandwidth of the transducer. The OFDM protocol is advantageous when it can have a wide spectrum range that can be divided into smaller frequency bands behaving as subcarriers. A certain frequency spread is allotted for the protocol to use and, if the physical channel is able to accommodate the required spectrum, a low BER will result due to carriers nor being lost due to being out of band.

It is also important to note that, even though the showcased results corresponded to an array with all of its channels

TABLE III

COMPARISON OF PMUT ACOUSTIC RECEIVER WITH
STATE-OF-THE-ART LONG RANGE DEVICES

Specification	This work	Commercial ¹
Range	2.7 m	$2-6 \ km$
Bandwidth	$200 \ kHz$	$18 \ kHz$
Frequency	$600 - 800 \ kHz$	9-27~kHz
Directivity	26^{o} 2	Omni-directional
Dimensions	$15x15x4 \ mm^{3}$	$10.2~cm \varnothing x~81.8~cm^{-3}$

- ¹ Based on [4]
- ² Angular width of main lobe where intensity is > 0 dBi (dB relative to isotropic emission). Directivity of PMUT arrays can be varied by varying the pitch of the elements in the array.

³ Dimensions include batteries

connected in parallel, the approach can also be used to read out single channels outputs for implementing DOA functionalities with PMUT arrays at similar distance ranges. This requires using charge amplifier circuits for each channel which was successfully tested for the same test setup, although smaller SNRs were obtained as there are fewer PMUT elements in parallel. However, the DOA functionalities do not require continuous bit transmission, but can rather be based on high power bursts that occur periodically with a low repetition frequency. This strategy can be used to compensate for the lower signal magnitude on individual channels.

IV. CONCLUSION

The current work was able to assess the possibility of enabling PMUT arrays as complete receiver elements for underwater acoustic networks at distances considerably larger than previously attempted for these kind of transducers. The large bandwidth the transducers offer, stemming from their inherently good acoustic matching to liquid media, was the key advantage explored.

Charge amplifier circuits were chosen for signal conditioning of the faint charges generated from acoustic signals at long distances. They were shown to have proper matching to the PMUT array's capacitive output while providing a large signal gain. The noise filtering capabilities of the circuit were also showcased, as well as the design flexibility of the pass-band frequencies and gains by variation of circuit values.

The packaging strategy chosen, by utilizing the flexible polymer PDMS, was effective in electrically isolating the MEMS devices and supporting circuitry without considerably impacting the acoustic performance. The PCB on which the circuits were supported also doubled as a mechanical structural layer for the delicate PMUT membrane chips. The resulting packaged device retained a small form factor, another defining advantage of PMUTs.

The feasibility of the devices as acoustic networking receivers at long distances was measured in terms of the SNR levels that can be obtained for burst signals and by implementing an actual communication protocol through the devices and characterizing the BER attainable for the corresponding SNRs. Both of the metrics showed the devices able to achieve high-throughput communication links at distances larger than 2 meters in scenarios such as a large tank and a pool that go beyond tightly controlled laboratory experiments. The BER

obtained $(10^{-2} - 10^{-3})$ are appropriate for telemetry data and image transmission, which fit the requirements of the proposed applications.

Scaling the array size is a possibility for enlarging the range. A larger number of elements would directly increase the signal level proportionally to the increased active area. The increased SNR would result in a corresponding decreased BER following the trend in Fig 7. The main sources of noise for the received signal are thermal noise in the conditioning circuitry and dielectric noise coming from the piezoelectric material [26]. An increased noise level would be introduced by the additional piezoelectric material and interconnects. It is expected that this increase would be small compared to the gain in signal level.

It is important to mention that the distances achieved are still far from the ranges achievable by large, bulk transducers such as in acoustic modems or pingers (Table III). In this context, it must be noted that these kind of links trade data throughput for the range they can achieve [5]. One reason for the lower throughput is the longer acoustic delays at larger distances, but limited bandwidth is a similarly significant factor. The decreased bandwidth is not only due to the low frequency of operation of the transducers but because of a less effective acoustic matching to the medium as compared to PMUTs (even bulk transducers operating at the same frequency as PMUTs suffer from a lower bandwidth).

The receivers detailed in this work would be mostly beneficial in an application that has links in a medium distance range and require a high communication speed, as they would take advantage from the larger bandwidth PMUTs provide. Such an application could potentially be medium range acoustic communication for coordination and mutual localization between Unmanned Autonomous Vehicles (UAVs) [27] in which the high data rates as well as the small footprint of the receivers would be beneficial.

The small form factor and possibility to integrate arrays of hundreds of PMUT elements is another distinctive characteristic that the discussed approach can offer. In this context, miniaturized devices with localization features could be implemented. An example envisioned application being handheld gadgets informing divers of their relative position to an acoustic beacon with dimensions much smaller than the current heavy and bulky underwater acoustic ranging systems.

Finally, even though the approach of this work was to explore the applicability of PMUT arrays as underwater receivers, it is worthwhile to mention that intra-body acoustic communication is an application that could clearly benefit from the approach taken in the present work. The miniaturized communication nodes would minimize how invasive they are while allowing large bandwidth, high-speed transmission. The improvement in SNRs at intra-body distances would also result in high BERs, further increasing the robustness of the communication links.

ACKNOWLEDGMENT

The authors would like to thank the staff of the George J. Kostas Nanoscale Technology and Manufacturing Research Center for assistance in device fabrication.

REFERENCES

- [1] B. Herrera et al., "PMUT-based high data rate ultrasonic wireless communication link for intra-body networks," presented at the Hilton Head Solid-State Sens., Actuators, Microsyst. Workshop, Hilton Head Island, SC, USA, Jun. 3-7, 2018.
- [2] F. V. Pop et al., "Novel pMUT-based acoustic duplexer for underwater and intrabody communication," in Proc. IEEE Int. Ultrason. Symp. (IUS), Oct. 2018, pp. 1-4.
- [3] C.-C. Kao, Y.-S. Lin, G.-D. Wu, and C.-J. Huang, "A comprehensive study on the Internet of underwater things: Applications, challenges, and channel models," Sensors, vol. 17, no. 7, p. 1477, Jun. 2017.
- Teledyne. (May 9, 2020). Acoustic Modems. [Online]. Available: http://www.teledynemarine.com/acoustic-modems/
- [5] EvoLogics. (May 9, 2020). Acoustic Modems. [Online]. Available: https://evologics.de/acoustic-modems
- [6] BlueRobotics. (May 9, 2020). Water Linked M64 Acoustic Modem. [Online]. Available: https://bluerobotics.com/store/comm-control-power/ acoustic-modems/wl-11003-1/
- [7] J. Cao, J. Liu, J. Wang, and X. Lai, "Acoustic vector sensor: Reviews and future perspectives," IET Signal Process., vol. 11, no. 1, pp. 1-9, Feb. 2017.
- WaterLinked. (May 9, 2020). Underwater Gps. [Online]. Available: https://waterlinked.com/underwater-gps/
- [9] Teledyne. (May 9, 2020). USBL Directional Acoustic Transponder (DAT). [Online]. Available: http://www.teledynemarine.com/usbl-dat? ProductLineID=59
- [10] Microflown. (Sep. 10, 2019). Sensor Node. [Online]. Available: http://microflown-avisa.com/hardware/amms-168/sensor-node/
- [11] Microflown. (Sep. 10, 2019). Acoustic Camera. [Online]. Available: https://www.microflown.com/assets/uploads/bestanden/Product-Leaflets/ Product-Leaflet_Acoustic-Camera.pdf
- [12] J. Kotus and G. Szwoch, "Calibration of acoustic vector sensor based on MEMS microphones for DOA estimation," Appl. Acoust., vol. 141,
- pp. 307–321, Dec. 2018.[13] W. Zhang, L. Guan, G. Zhang, C. Xue, K. Zhang, and J. Wang, "Research of DOA estimation based on single MEMS hydrophone," Sensors, vol. 9, no. 9, pp. 6823-6834, Aug. 2009.
- [14] Y. Lu and D. A. Horsley, "Modeling, fabrication, and characterization of piezoelectric micromachined ultrasonic transducer arrays based on cavity SOI wafers," J. Microelectromech. Syst., vol. 24, no. 4, pp. 1142-1149,
- [15] E. Demirors et al., "The SEANet project: Toward a programmable Internet of underwater things," in Proc. 4th Underwater Commun. Netw. Conf. (UComms), Aug. 2018, pp. 1-5.
- [16] R. J. Przybyla, H.-Y. Tang, A. Guedes, S. E. Shelton, D. A. Horsley, and B. E. Boser, "3D ultrasonic rangefinder on a chip," IEEE J. Solid-State Circuits, vol. 50, no. 1, pp. 320-334, Jan. 2015.
- [17] X. Jiang et al., "Monolithic ultrasound fingerprint sensor," Microsyst. Nanoeng., vol. 3, no. 1, p. 17059, Dec. 2017.
- [18] D. E. Dausch, K. H. Gilchrist, J. B. Carlson, S. D. Hall, J. B. Castellucci, and O. T. von Ramm, "In vivo real-time 3-D intracardiac echo using PMUT arrays," IEEE Trans. Ultrason., Ferroelectr., Freq. Control,
- vol. 61, no. 10, pp. 1754–1764, Oct. 2014. [19] Chirp. (Oct. 9, 2019). Ultrasonic Time Of Flight Sensing. [Online]. Available: http://www.chirpmicro.com/
- [20] B. Herrera, F. Pop, C. Cassella, and M. Rinaldi, "PMUT-enabled underwater acoustic source localization system," in Proc. IEEE Int. Ultrason. Symp. (IUS), Oct. 2019, pp. 1103-1106.
- [21] S. Sadeghpour, M. Kraft, and R. Puers, "Highly efficient piezoelectric micromachined ultrasound transducer (PMUT) for underwater sensor networks," in Proc. 20th Int. Conf. Solid-State Sensors, Actuat. Microsyst. Eurosensors XXXIII (TRANSDUCERS EUROSEN-SORS XXXIII), Jun. 2019, pp. 162-165.
- [22] S. K. E. Hansen, "Design and experimental investigation of charge amplifiers for ultrasonic transducers," M.S. thesis, Dept. Phys. Technol., UiT Norges arktiske universitet, Tromsø, Norway, 2014.
- [23] H.-Y. Tang et al., "3-D ultrasonic fingerprint sensor-on-a-chip," IEEE
- J. Solid-State Circuits, vol. 51, no. 11, pp. 2522–2533, Nov. 2016.
 [24] E. Research. (Jul. 26, 2020). N210 Gps. [Online]. Available:
- https://www.ettus.com/all-products/un210-kit/
 [25] P. Laugier and G. Haïat, "Introduction to the physics of ultrasound," in Bone Quantitative Ultrasound. Dordrecht, The Netherlands: Springer, 2011, pp. 29-45.
- [26] R. J. Littrell, "High performance piezoelectric MEMS microphones," Ph.D. dissertation, Univ. Michigan, Ann Arbor, MI, USA, 2010.
- [27] G. E. Burrowes and J. Y. Khan, "Short-range underwater acoustic communication networks," in Autonomous Underwater Vehicles, N. A. Cruz, Ed. Rijeka, Croatia: IntechOpen, 2011, pp. 173-198.



Bernard Herrera (Graduate Student Member, IEEE) received the B.Sc. degree in electrical engineering from the Universidad San Francisco de Quito, Ecuador, in 2011, and the M.Sc. degree in electrical and computer engineering from Northeastern University, as a Fulbright Scholar, in 2017, where he is currently pursuing the Ph.D. degree with the Northeastern Sensors and Nano Systems Laboratory, under the supervision of Prof. M. Rinaldi. During his studies, he did an exchange year at the University of Illinois at Urbana-Champaign, USA,

where he also performed as a Research Assistant. He then joined the Universidad San Francisco de Quito, as an Instructor and a Researcher. His research currently focuses on piezoelectric micromachined ultrasonic transducers with intra-body and underwater applications.



Flavius Pop (Graduate Student Member, IEEE) received the B.Sc. and M.Sc. degrees in electrical engineering from the University of Udine, Italy, in 2014 and 2016, respectively. He is currently pursuing the Ph.D. degree with the Northeastern Sensors and Nano Systems Laboratory, Northeastern University, under the supervision of Prof. M. Rinaldi. During his master studies, he was an international exchange student (ERASMUS) for one year at ESIEE Paris, France, from 2014 to 2015. Following, he was a Visiting Research Fellow with

The University of Tokyo (TODAI), Japan, for six months in 2015, working on Atomic Force Microscopes (AFM). For his master's thesis, he was a Visiting Research Fellow with Carnegie Mellon University (CMU), Pittsburgh, PA, USA, for one year in 2016, working on lithium niobate (LN) MEMS resonators for RF applications. His research currently focuses on piezoelectric micromachined ultrasonic transducers (pMUTs) for intrabody and underwater communication links and bio sensing applications.



Cristian Cassella (Member, IEEE) received the B.S.E. and M.Sc. degrees (Hons.) from the University of Rome Tor Vergata, Rome, Italy, in 2006 and 2009, respectively, and the Ph.D. degree from Carnegie Mellon University, Pittsburgh, PA, USA, in 2015. In 2011, he was a Visiting Scholar with the University of Pennsylvania, Philadelphia, PA, USA. In 2015, he was a Post-Doctoral Research Associate with Northeastern University, Boston, MA, USA. In 2016, he became an Associate Research Scientist. He is currently an Assistant Professor with the

Electrical and Computer Engineering Department, Northeastern University. He is the author of 55 publications in peer-reviewed journals and conference proceedings. He holds two patents and three patent applications in the areas of MEM-resonators and RF systems. He was a recipient of the Best Paper Award at the 2013 IEEE International Frequency Control Symposium, Prague. In 2018, he was awarded by the European Community (EU) the prestigious Marie-Sklodowska-Curie Individual Fellowship. Two of his peer-reviewed journal articles published in the IEEE JOURNAL OF MICROELECTROMECHANICAL SYSTEMS (JMEMS) were selected as Papers of Excellent Quality (JMEMS RightNowPapers), hence being released as open access. One of his journal articles was chosen as the cover for the Nature Nanotechnology October 2017 issue. He is also a Technical Reviewer of several journals, such as Applied Physics Letters, the IEEE JOURNAL OF MICROELECTROMECHANICAL SYSTEMS, the IEEE ELECTRON DEVICE LETTERS, the Journal of Micromechanics and Microengineering, Journal of Applied Physics, the IEEE SENSORS LETTERS, the IEEE TRANSACTIONS ON ELECTRON DEVICES, and the Review of Scientific Instruments.



Matteo Rinaldi (Senior Member, IEEE) received the Ph.D. degree in electrical and systems engineering from the University of Pennsylvania, Philadelphia, PA, USA, in December 2010. He was a Post-Doctoral Researcher with the University of Pennsylvania in 2011. In January 2012, he joined as an Assistant Professor the Electrical and Computer Engineering Department, Northeastern University, Boston, MA, USA, where he is currently an Associate Professor and the Director of Northeastern SMART, a University Research Center that, by fos-

tering partnership between university, industry, and government stakeholders, aims to conceive and pilot disruptive technological innovation in devices and systems capable of addressing fundamental technology gaps in several fields, including the Internet of Things (IoT), 5G, quantum engineering, digital agriculture, robotics, and healthcare. His group has been actively working on experimental research topics and practical applications to ultra-low power MEMS/NEMS sensors (infrared, magnetic, chemical, and biological, plasmonic micro- and nano-electromechanical devices, medical microsystems

and implantable microdevices for intra-body networks, reconfigurable radio frequency devices and systems, phase change material switches, and 2-D material enabled micro- and nano-mechanical devices). His group's research was supported by several Federal grants (including DARPA, Advanced Research Projects Agency-Energy, the National Science Foundation (NSF), and the Department of Homeland Security), the Bill and Melinda Gates Foundation, and the Keck Foundation with funding of more than \$14 M since 2012. He has coauthored more than 130 publications in the aforementioned research areas. He also holds eight patents and more than ten device patent applications in the field of MEMS/NEMS. He was a recipient of the IEEE Sensors Council Early Career Award in 2015, the NSF CAREER Award in 2014, and the DARPA Young Faculty Award in the class of 2012. He received the Best Student Paper Award at the 2009, 2011, 2015 (with his student), and 2017 (with his student) IEEE International Frequency Control Symposiums, the Outstanding Paper Award at the 18th International Conference on Solid-State Sensors, Actuators and Microsystems, Transducers 2015 (with his student), and the Outstanding Paper Award at the 32nd IEEE International Conference on Micro Electro Mechanical Systems, MEMS 2019 (with his student).